Identifying watershed-scale barriers to groundwater flow: Lineaments in the Canadian Shield

Tom Gleeson[†]
Kent Novakowski
Civil Engineering Department, Queen's University, Kingston, Ontario K7L 3N6, Canada

ABSTRACT

Lineament identification is a standard but controversial hydrogeologic practice. In this study, we present a rigorous examination of the hydrology of lineaments in a crystalline bedrock setting. Lineaments are reinterpreted as watershed-scale hydraulic barriers, in contrast to previous interpretations as fractured conduits that focus recharge and flow. In the study area, an ~900 km^2 watershed underlain by the granitic and gneissic terrain of the Canadian Shield, bedrock lineaments are associated with linear lake shores and perennial wetland complexes. Lineaments were identified using a robust multi-image method and characterized by remote sensing, fracture mapping, drilling, hydraulic characterization, and numerical simulation of a coupled groundwater–surface-water system. Results indicate that two principal lineament sets are oriented parallel to fracture and fault orientations, and thus lineaments are interpreted as structural features, either fault zones or fracture zones with limited displacement. Faulted lineaments are more effectively identified by digital elevation model (DEM) topographic data rather than Landsat tonal imagery. Hydrogeological characterization and geomatic data indicate that the fractured bedrock underlying lineaments is composed of poorly connected zones of reduced permeability due to fault zone and/or fluid flow processes. Field data and numerical simulations suggest that lineament areas are barriers to recharge and flow in this setting as a result of permeability reduction. Integrated data sets and models of lineament permeability that are geologically realistic result in a better understanding of fractured bedrock aquifers and patterns of fluid flow in the brittle uppermost crust.

[†]E-mail: tom@ce.queensu.ca

Keywords: hydrogeology, structural geology, environmental geology, remote sensing, lineaments, faults, hydraulic barriers.

INTRODUCTION

Bedrock aquifers are complex hydrogeological systems that are essential for water resources and contaminant disposal around the world (Edet et al., 1998; Magowe and Carr, 1999; Flint et al., 2001; Berkowitz, 2002; Caine and Tomusiak, 2003; Sener et al., 2005; Shaban et al., 2006). Identification and characterization of structures that control watershed-scale groundwater flow are essential for both groundwater management and understanding fluid flow in bedrock aquifers (Ferrill et al., 2004; Seaton and Burbey, 2005; Denny et al., 2007). Lineaments are extensive linear surface features and the surface expression of fracture zones, faults, or geological contacts (O'Leary et al., 1976; Prost, 1994; Jackson, 1997; Singhal and Gupta, 1999). Lineament identification is standard practice in fractured rock hydrogeology, though it is also controversial and periodically questioned by hydrogeologists and structural geologists (Wise, 1982). This study presents a necessary and rigorous examination of the hydrology of lineaments within the context of the current understanding of fault hydrology. Lineament identification is defensible when multiple observers use multiple image types, classify lineaments by significance, and cull observations that do not meet reproducibility criteria (Mabee et al., 1994; Sander et al., 1997; Singhal and Gupta, 1999; Tam et al., 2004). Lineament identification is a useful hydrogeologic tool when lineaments are identified with a defensible and reproducible method and analyzed with supplementary geomatic, geologic, and hydrogeologic data within a well-documented structural geology framework.

Early studies suggested that lineaments were associated with higher water well yields, although the number of studied wells was small (Lattman and Parizek, 1964; Lattman and Matzke, 1971; Siddiqui and Parizek, 1971). Consulting hydrogeologists and researchers often continue to assume a priori that lineaments are fractured recharge and flow conduits with high groundwater potential (e.g., Krishnamurthy et al., 2000; Sener et al., 2005; Shaban et al., 2006). However, lineaments do not correlate with well yields, or only lineaments with certain characteristics correlate to well yields, but these correlations are not consistent across different geological, topographic, and geomorphic settings (Waters et al., 1990; Gustafsson, 1994; Mabee et al., 1994, 2002; Sander et al., 1997; Edet et al., 1998; Mabee, 1999; Magowe and Carr, 1999; Moore et al., 2002; Solomon and Quiel, 2006; Sander, 2007). Therefore, the assumption that lineaments are fractured conduits is not consistent with much of the well yield data around lineaments.

To our best knowledge, lineaments have not previously been examined using recent models of fault architecture and permeability. Fault zones are conceptualized as fault cores and flanking damage zones that crosscut an undeformed protolith (Caine et al., 1996). Permeability is typically reduced in fault cores due to brecciation, cataclasis, and clay-rich gouge zones (Evans, 1988; Goddard and Evans, 1995; Caine and Forster, 1999). In crystalline rocks, the permeability of the damage zone is often higher than the protolith due to fracture networks, which can be infilled by mineral precipitation during or after deformation, reducing permeability (Evans et al., 1997; Rawling et al., 2001). The fault core and surrounding damage zone result in an anisotropic permeability structure that is a hydraulic conduit, barrier, or conduit-barrier system, depending on the fault-zone architecture and direction of flow examined (Forster and Evans, 1991; Caine and Forster, 1999; Caine and Tomusiak, 2003; Bense and Person, 2006). The permeability, width, and anisotropy of a damage zone and fault core can be extremely heterogeneous along strike (Evans and Chester, 1995; Caine and Forster, 1999; Fairley and

GSA Bulletin; March/April 2009; v. 121; no. 3/4; p. 333–347; doi: 10.1130/B26241.1; 10 figures; 2 tables.

Hinds, 2004; Minor and Hudson, 2006) and vary during deformation (Chester et al., 1993). For watershed-scale groundwater flow, high-permeability structures are recharge and flow conduits that can increase subsurface connectivity (Mayer and Sharp, 1998; Flint et al., 2002; Denny et al., 2007); low-permeability barriers restrict recharge and flow and can compartmentalize flow systems (Marler and Ge, 2003; Seaton and Burbey, 2005); and conduit-barriers can have complex behavior such as compartmentalizing lateral flow while allowing significant vertical flow or recharge (Ferrill et al., 2004; Bense and Person, 2006). The complexity of permeability patterns in field-based, fault architecture models suggests that the assumption that lineaments are fractured conduits may be too simplistic.

In this study, a preliminary inspection of a watershed underlain by granitic and gneissic terrain of the Canadian Shield suggests that lineaments are associated with linear lake shores and perennial wetland complexes. The perennial nature of the surface-water bodies suggests that water infiltration is limited rather than enhanced in lineament areas, possibly due to subsurface permeability. The objective of this study was to determine if lineaments are structurally controlled, hydraulic barriers to groundwater recharge and flow in this geological setting. Lineaments were identified using a defensible, remote-sensing method and analyzed using supplementary geomatic data. Mapped fracture patterns provided constraints for the structural geometry of lineaments. The relationship between surface water and groundwater was characterized in detail at a representative lineament. Finally, a synthetic domain representing a typical lineament was simulated to reveal the significance of hydraulic conductivity and fracture aperture in the observed surface-water and groundwater systems. This paper is an important example of applying remote sensing and geomatics to a complex hydrogeologic problem, as has been called for in recent reviews (Becker, 2006; Brunner et al., 2007). Since lineaments are surface expressions of subsurface phenomena, and they are common on Earth's surface, examinations of lineaments using rigorous and defensible methods from multiple disciplines may aid the study of other hydrogeologic and geologic problems.

REGIONAL GEOLOGY AND HYDROLOGY

The ~900 km^2 Tay River watershed is located in rural eastern Ontario, Canada (Fig. 1). The watershed is characterized by an undulating upland area underlain by Precambrian rocks

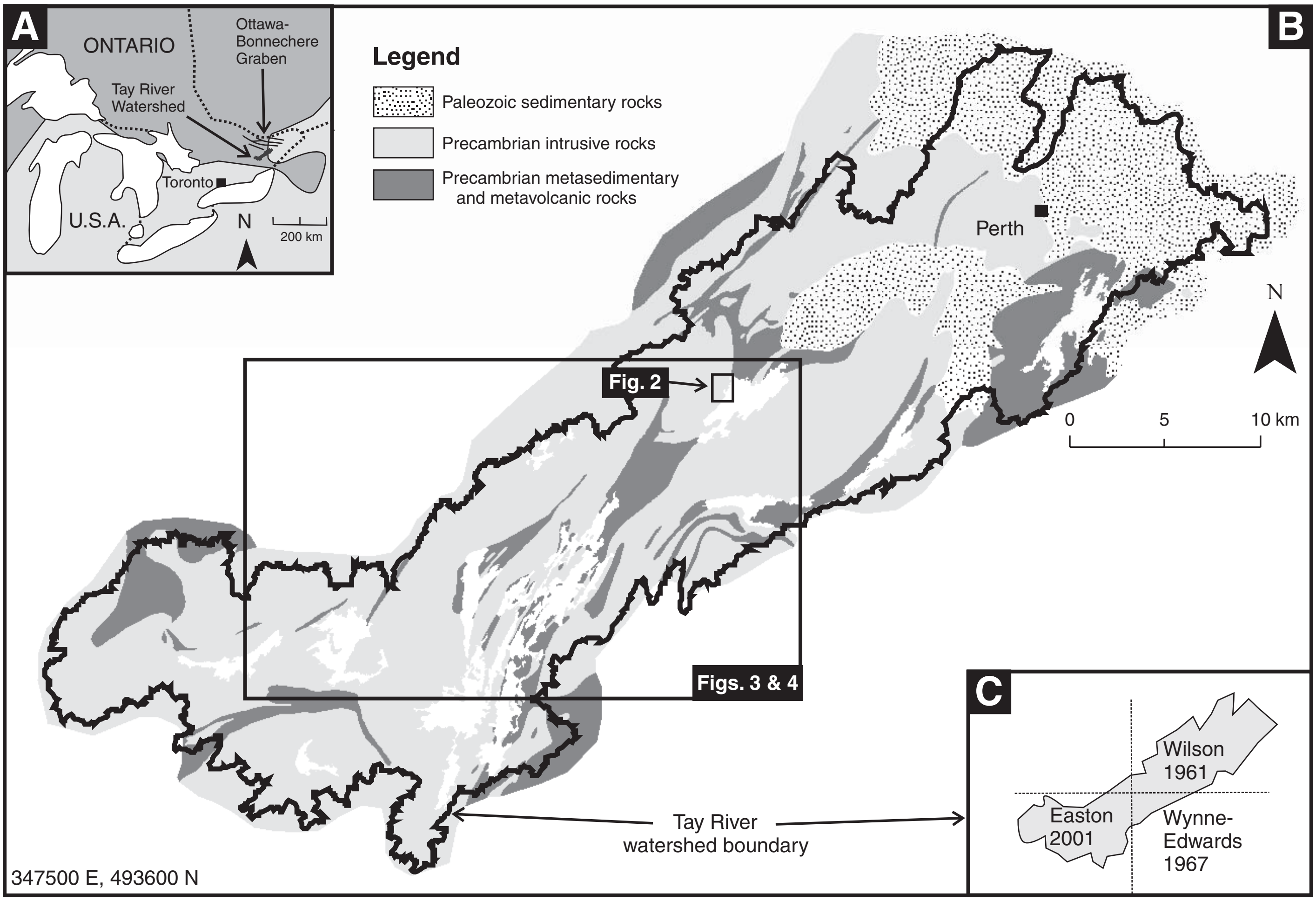

Figure 1. (A) Tay River watershed study location in Ontario, Canada. Dark gray indicates Precambrian rocks; light gray indicates Paleozoic rocks; Ottawa-Bonnechere graben is shown for reference. (B) Simplified geological map of the Tay River watershed derived from existing Geological Survey of Canada and Ontario Geological Survey maps. Individual rock types are grouped together into hydrogeologically significant units. (C) Index of map sources for geological compilation (Wilson, 1961; Wynne-Edwards, 1967; Easton 2001).

and a topographically subdued downstream area underlain by Paleozoic sedimentary rocks. This study is focused on the bedrock geology and hydrogeology of the Precambrian terrain. The Precambrian units are upper greenschist– to granulite metamorphic–grade metasediments and metavolcanics with associated intrusive rocks of the Frontenac and Sharbot Lake terranes of the Grenville Province (Culotta et al., 1990; Easton, 1992). Metasedimentary and metavolcanic rocks are strongly foliated and consist of marble, dolomite, siliciclastic and quartzofeldspathic gneiss, and felsic to intermediate metavolcanics. Weakly to strongly foliated intrusive rocks include granodiorite, granite, diorite, syenite, migmatite, and minor mafic intrusive rocks (gabbro, anorthosite, and norite). Flat-lying Paleozoic sandstone, dolomite, and dolomitic limestone locally overlie Precambrian units. Complex ductile fabric orientations are locally common in Precambrian units, but the predominant structural and metamorphic grain consistently strikes northeast (Wilson, 1961; Davidson and Ketchum, 1993; Easton, 2001).

The Ottawa-Bonnechere graben is a Tertiary northwest-trending normal fault system that defines significant topographic features north of the study area (Fig. 1A; Kay, 1942). The graben is considered to be a Neoproterozoic failed arm of a triple junction that was repeatedly reactivated by Phanerozoic tectonism (Kumarapeli, 1978, 1981; Rimando and Benn, 2005). The southern half of the graben is characterized by north-facing topographic breaks with down-thrown north-side hanging walls. Joint orientations in the regions surrounding the faults are predominantly parallel to fault orientations, which is consistent with joint development during normal faulting. Although the Tay River watershed is south of the area mapped by Kay (1942), the southernmost fault of the Ottawa-Bonnechere graben is interpreted to extend through the central Tay River watershed (Plate 6 *in* Kay, 1942).

The surficial geology of the study area is composed of a thin (<1 m) and discontinuous till veneer with littoral or organic deposits adjacent to surface-water bodies (Kettles, 1992). The discontinuous till veneer rarely masks the structure of the underlying bedrock. The coarse-grained littoral and organic deposits are limited in extent and thickness (1–5 m). Glacial striae and drumlins indicate that the predominant ice-flow direction was south-southwestward (Kettles, 1992). Surficial mapping and residential water well records indicate that unconsolidated materials do not provide significant groundwater potential and are therefore not the focus of this study.

Results from bedrock geological mapping conducted by the Geological Survey of Canada and Ontario Geological Survey were compiled and simplified into hydraulically significant lithologic groups in Figure 1, following Caine and Tomusiak (2003). Individual rock units were reclassified under the assumption that rock types with similar geologic history and response to brittle deformation should exhibit similar hydrogeological properties at the watershed scale (Caine and Tomusiak, 2003). The hydrogeological consistency of the amalgamated rock groups was evaluated using the specific capacity of residential water wells (MOE, 2006). Specific capacity was derived from drawdown data during 1 h pumping tests conducted after well completion (Freeze and Cherry, 1979). Null (i.e., no drawdown during pumping) and spurious (i.e., drawdown greater than depth of well) specific capacity values were removed from the database. Wells completed in metasedimentary and metavolcanic rocks ($n = 383$) and intrusive rocks ($n = 749$) had a mean specific capacity of 2.3×10^{-5} m^3 s^{-1} m^{-1} and 3.0×10^{-5} m^3 s^{-1} m^{-1}, respectively. For comparison, wells completed in sedimentary rocks ($n = 357$) had a mean specific capacity of 7.3×10^{-5} m^3 s^{-1} m^{-1}. The similarity of specific capacity in Precambrian units suggests that they have similar hydrogeological characteristics at the watershed scale (Singer et al., 2003).

Regional groundwater flow in the Tay River watershed is toward the northeast, parallel to the Tay River, and the approximate groundwater gradient is 0.001 (Golder Associates Ltd., 2003). At a local scale, groundwater–surface-water interactions and recharge processes have been examined at a site far from mapped lineaments (Praamsma, 2006; Milloy, 2007). Hydraulic testing coupled with hydraulic head measurements revealed that recharge is limited to ~1% of precipitation (Milloy, 2007). No attempt to predict the location of recharge features or understand the role of lineaments was undertaken in these studies.

The areas underlain by Precambrian rocks are characterized by subdued (<200 m) yet heterogeneous and hummocky topography with complex surface-water patterns due to the glacial history. The Tay River watershed consists of over 3000 permanent surface-water features. The size and type of surface water features vary from >10 km^2 lakes to <100 m^2 vernal ponds. Linear lake shores and wetland complexes are commonly persistent over kilometers. Extremely high surface-water gradients between adjacent surface-water features suggest poor subsurface connectivity. The numerous lakes and wetlands in the Tay River watershed are important and characteristic hydrographic features in the watershed, similar to other areas of the Canadian Shield (Farvolden et al., 1988).

METHODS

The study examined two scales. At the watershed scale, geological, remote sensing, and water well data were integrated into a geomatic database to identify and analyze lineaments. At a local scale, a lineament, representative in length, orientation, topography, surface-water gradient, and specific capacity, was characterized using hydrogeological and numerical modeling tools.

Geomatics

In this study, lineaments were defined as linear tonal and/or topographic features with a minimum length of 500 m. The methodology of lineament identification generally followed Mabee et al. (1994) and is summarized in the Appendix. The potential hydraulic importance of lineaments was explored using the culled specific capacity database for residential water wells, described already (MOE, 2006). For the analysis, only wells completed in Precambrian units ($n = 1132$) were used. The culled database was interpolated using kriging and an inverse weighted distance function. Interpolation using the two methods was compared visually and qualitatively using raster mathematics to recognize any systematic trends due to the interpolation method. The interpolated values were then visually compared to the distribution of identified lineaments.

Hydraulic barriers typically have hydraulic head discontinuities or high hydraulic gradients oblique to the structure (Bense and Person, 2006). The relative paucity of high-quality hydraulic head measurements near lineaments in the study area precludes an analysis of groundwater gradients. However, in a well-connected groundwater–surface-water system, surface-water features are also manifestations of the water table (Fredrick et al., 2007). Therefore, if lineaments are permeable features with high connectivity, the surface-water gradients around lineaments are expected to be low. Surface-water gradients were mapped by manually compiling digital elevation model (DEM) surface elevations for all permanent water bodies. The potential gradient between adjacent surface-water bodies was mapped by first creating a triangulated irregular network of interpolated elevations between surface-water features.

Twenty lineaments representing the various geological and physiographic settings and lineament orientations were verified by field ground-truth during the spring, summer, and fall of 2006 to ensure that surface-water features were perennial. The physiographic expression, wetland classification, and nearby outcrops (see next section) were inspected during field work.

Fracture Mapping

Lineaments in topographically subdued areas typically occurred in wet, low-lying areas with little exposed outcrop, which is a challenge for structural analysis (Isachsen, 1976; Spitzer, 1981; Wise et al., 1985). Therefore, fractures were measured and characterized at 13 outcrops both adjacent to and in-between mapped lineaments. Outcrops with two near-orthogonal faces were preferred to avoid orientation bias (La Pointe and Hudson, 1985). Observations typically included fracture orientation, length, and termination style (abutting, blind, or through-going). The orientation and type of foliation were also recorded. A 180 m scan line (TG06–07 on Fig. 2) was completed on an unusually well-exposed outcrop adjacent to the lineament described in detail next, herein called the "Christie Lake lineament." Fracture measurements from the scan line were corrected for orientation bias using Terzaghi's (1965) method. Fracture and foliation measurements from other outcrops were not corrected for orientation bias because the outcrops did not have a systematic trend.

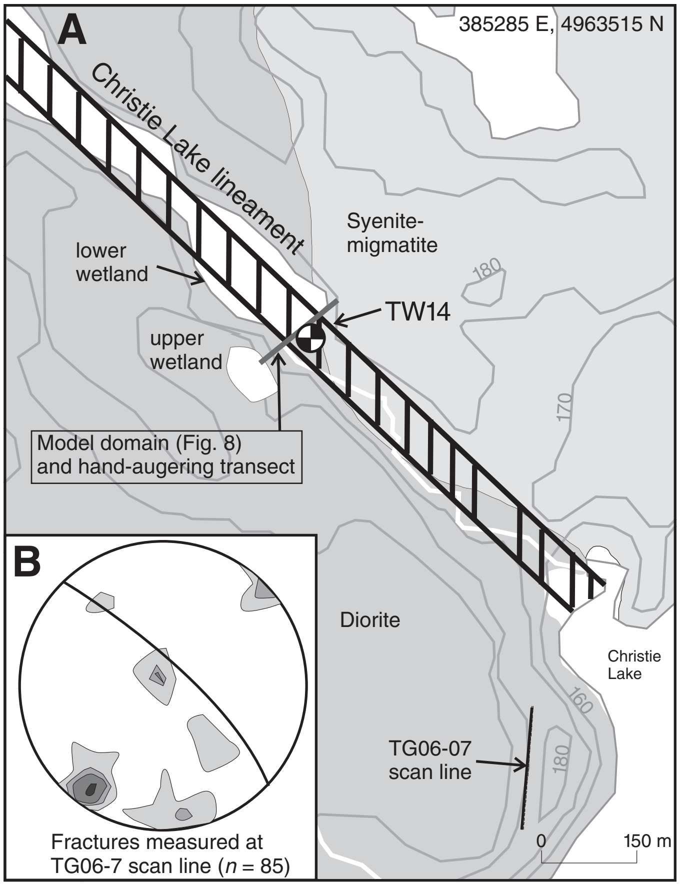

Figure 2. (A) Christie Lake study site with bedrock geology from Wilson (1961). The Christie Lake lineament, originally mapped as a fault truncating units to the northwest, is shown as 100-m-wide zone oriented 310° bisecting a linear wetland complex. Borehole TW14 is located in the center of the lineament. The locations of cross-sectional model domain (Fig. 8) and hand-augering transect described in the text are also shown. (B) Equal-area, lower-hemisphere stereonet projection of poles to fractures measured at the nearby TG06–07 scan line, plotted with 2σ uncertainty. The mean orientation (305/80) of fractures is also plotted for comparison to the lineament orientation.

Hydrogeological Characterization

The 3-km-long, northwest-trending "Christie Lake lineament" bisects a wetland complex, herein called the "lower wetland," and it is mapped as a fault of unknown displacement that truncates units to the northwest (Fig. 2; Wilson, 1961). The lineament is a topographic break where elevation increases to the southwest. A number of wetlands are found in the upland area to the southwest, including the swamp herein called the "upper wetland" (Fig. 2). The Christie Lake lineament was characterized in detail because it is representative of lineaments in the study area in length, orientation, and physiography.

A monitoring well (TW14; 0.152 m diameter) was drilled in the middle of the lineament to a depth of 44 m below the ground surface. Drilling chips sampled from discrete depths were tested for the presence of carbonate using dilute hydrochloric acid to determine the vein mineralogy. Well TW14 was characterized using a downhole camera and via hydraulic testing at 1.77 m test intervals isolated by straddle packers. Slug tests were completed in each interval using 5 L of water and analyzed using the Hvorslev (1951) method as described in Butler (1998). Measured transmissivities were converted to hydraulic conductivities and single-fracture effective apertures for each interval (Novakowski et al., 2007). Two slotted, 0.051-m-diameter multilevel piezometers set in #2 sand were installed in the transmissive zones of TW14 and separated by >3 m of bentonite. The upper portion of the well was left open, resulting in three discrete piezometer intervals (TW14S, TW14M, and TW14D). Each piezometer was developed until groundwater was not turbid by pumping for 1–2 h. Pressure transducers were installed in the upper and lower piezometer and the adjacent lower wetland. Hydraulic head data were recorded at 15 min intervals for 3 months to constrain possible hydraulic connections between surface-water features and the subsurface intervals.

Ten shallow boreholes were drilled until refusal using a hand auger along a 20 m transect perpendicular to the lineament to evaluate the properties of the unconsolidated material in the lower wetland. Intact core was removed from the hand auger and logged at 0.1 m intervals using the Unified Soil Classification System (American Society for Testing and Materials, 2007).

Numerical Simulations of Surface-Water–Groundwater Interactions

HydroGeoSphere, a finite-element, coupled groundwater and surface-water model was used to explore local-scale interactions between surface water and groundwater in this fractured rock terrain (Therrien and Sudicky, 1996; Therrien et al., 2006). *HydroGeoSphere* was used because it is a reliable simulator of variably saturated conditions and groundwater–surface-water interactions and has been proven accurate for a variety of geologic settings and spatial and temporal scales (Cey et al., 2006; Park et al., 2008). A synthetic cross-sectional domain was built that was physically consistent to both the Christie Lake lineament site and other lineaments in the study area. The topographic gradient (0.4) was based on a detailed global positioning system (GPS) topographic corrected with the wide area augmentation system of the area surrounding these two perennial wetland areas (cross section located on Fig. 2). The model domain was a 100 × 50 × 1 m cross section discretized into 39,000 nodes with 0.5 m spacing at the bottom grading finer toward the surface, where the main head and flux dynamics occur. No flow boundaries were applied along the lateral and bottom boundaries of the domain to enable examination of groundwater–surface-water interactions without additional complicating influences (Panday and Huyakorn, 2004). The robustness of the flow solution was tested using more discretized grids. Transient simulations were run until steady-state conditions were derived (1–30 yr in model time), with a maximum allowable water balance error of 1% of inflow.

The domain was simulated using both equivalent porous media and discrete fracture network approaches to constrain possible bulk hydraulic conductivity values or fracture apertures, respectively. For the equivalent porous media approach, it was assumed that the hydraulic conductivity tensor was isotropic and homogeneous. For the discrete fracture domain, an orthogonal fracture network was implemented because of observed fracture patterns (see Results). The assigned values of hydraulic conductivity and fracture aperture are discussed later because they were derived from hydraulic testing results.

Since surface and subsurface flow is explicitly coupled in *HydroGeoSphere*, rainfall either directly ran off through a critical depth boundary (exiting the domain at the lowest topographic point), ponded in the topographic depressions, or infiltrated the domain. The rainfall pathway was dependent on subsurface permeability (bulk hydraulic conductivity and fracture aperture) as well as overland flow and evapotranspiration parameters. Overland flow and evapotranspiration parameters were derived from Randall (2005), who simulated a similar geologic and physiographic setting. A long-term mean annual rainfall of 0.9 m/yr was applied to the surficial nodes (Golder Associates Ltd., 2003). Simulations were completed with and without evapotranspiration to evaluate the importance of this parameter.

Depth of water in the upper wetland was considered the primary fitting parameter because, in the absence of a dense network of monitoring wells, it was the most sensitive and hydraulically significant parameter to changes in hydraulic conductivity and fracture aperture. The maximum depth of water in the upper wetland was 2 m in the model domain. At greater depths, overland flow toward the lower wetland was initiated. Numerical simulations indicated that the depth of water in the upper wetland was reproducible to 0.1 m. This modeling exercise is considered to be a useful numerical experiment for testing conceptual models of groundwater–surface-water interactions because numerous subsurface targets are not available for calibration and verification.

RESULTS

Lineament Identification and Analysis

A greater number of lineaments was repeatedly observed using the Landsat imagery (111) than with the DEM (78). Landsat-derived lineaments have a unidirectional northeast orientation and linear directional mean of 042° (Fig. 3A). This trend is coincident with lineaments derived from a different Landsat image by an independent study (Andjelkovic and Cruden, 1998), indicating that lineament detection is a robust and reproducible technique if completed systematically (Fig. 3). DEM-derived lineaments have bidirectional northeast and northwest orientation, with linear directional means of 033° and 312°, respectively (Fig. 3B). For both DEM and Landsat mediums, selected lineaments were also observed in aerial photographs and targeted ground truthing. Every observed lineament was related to a surface-water feature (e.g., a linear lake shore, wetland complex, or river reach). Field observations indicated that the wetlands associated with lineaments were perennial rather than vernal. Although Landsat highlights tonal differences and the DEM highlights topographic differences, the same lineaments were often detected on both DEM and Landsat. The shared lineaments typically also shared characteristics (scale detected and linearity), suggesting that lineaments in this study are tonal-topographic features. Therefore, both data types are considered useful, but as discussed next, lineament detection using DEM data may be more valuable in identifying structural discontinuities in a topographically subdued landscape.

The specific capacity database was analyzed to examine permeability trends in lineaments areas. The database was interpolated using kriging and inverse weighted distance functions. For kriging, a spherical variogram model was chosen based on visual best fit with a resultant range and sill of 800 m and 350 (L min^{-1}m^{-1})^2, respectively. No systematic differences were observed when the results for the two interpolation methods were compared visually and qualitatively using raster mathematics. Figure 4A illustrates the interpolation using the inverse weighted method and the distribution of DEM-derived lineaments. The specific capacity of residential wells completed in Precambrian rock was not higher near lineaments at a watershed scale. Detailed spatial analysis indicates that specific capacity may actually increase with distance from lineaments and is definitely higher in areas distal to lineaments compared to areas within 250 m of lineaments (Table 1).

TABLE 1. SPECIFIC CAPACITY OF WATER WELLS AT VARIOUS DISTANCES FROM DIGITAL ELEVATION MODEL (DEM)–DERIVED LINEAMENTS

Distance from lineament (m)	Number of wells	Specific capacity (L min^{-1} m^{-1})
25	11	1.4 ± 2.5
50	23	1.2 ± 2.3
100	124	1.7 ± 5.8
250	179	1.7 ± 5.6
All wells in watershed	1132	2.36 ± 7.8

Figure 4B depicts the potential gradient between adjacent surface-water features and the location of DEM-derived lineaments not associated with lake shores. Lineaments associated with lake shores are not included because the gradient at a lake shore is zero by definition. Generally, lineaments are coincident with higher potential surface-water gradients. If lineaments are well-connected, high-permeability features, the surface-water and groundwater gradients would be relatively low. The correlation of lineaments with high potential surface-water gradients and lower specific capacity indicates that lineaments are less-permeable features that may be regional hydraulic barriers.

Fracture Mapping

At a watershed scale, three fracture sets are generally observed (Fig. 5A). The most prominent is the steep to vertical, northwest-striking set (306/83 mean orientation calculated as the great circle normal to highest concentration of fracture poles), which are typically throughgoing and greater than 5 m in length. The northwest set parallels the fracture set related to the Ottawa-Bonnechere graben, which is interpreted to have developed during normal faulting (Kay, 1942). The second fracture set is a steep, northeast-striking (039/79 mean orientation) set, which are typically throughgoing or abutting and less than 5 m in length. The northeast set parallels the metamorphic

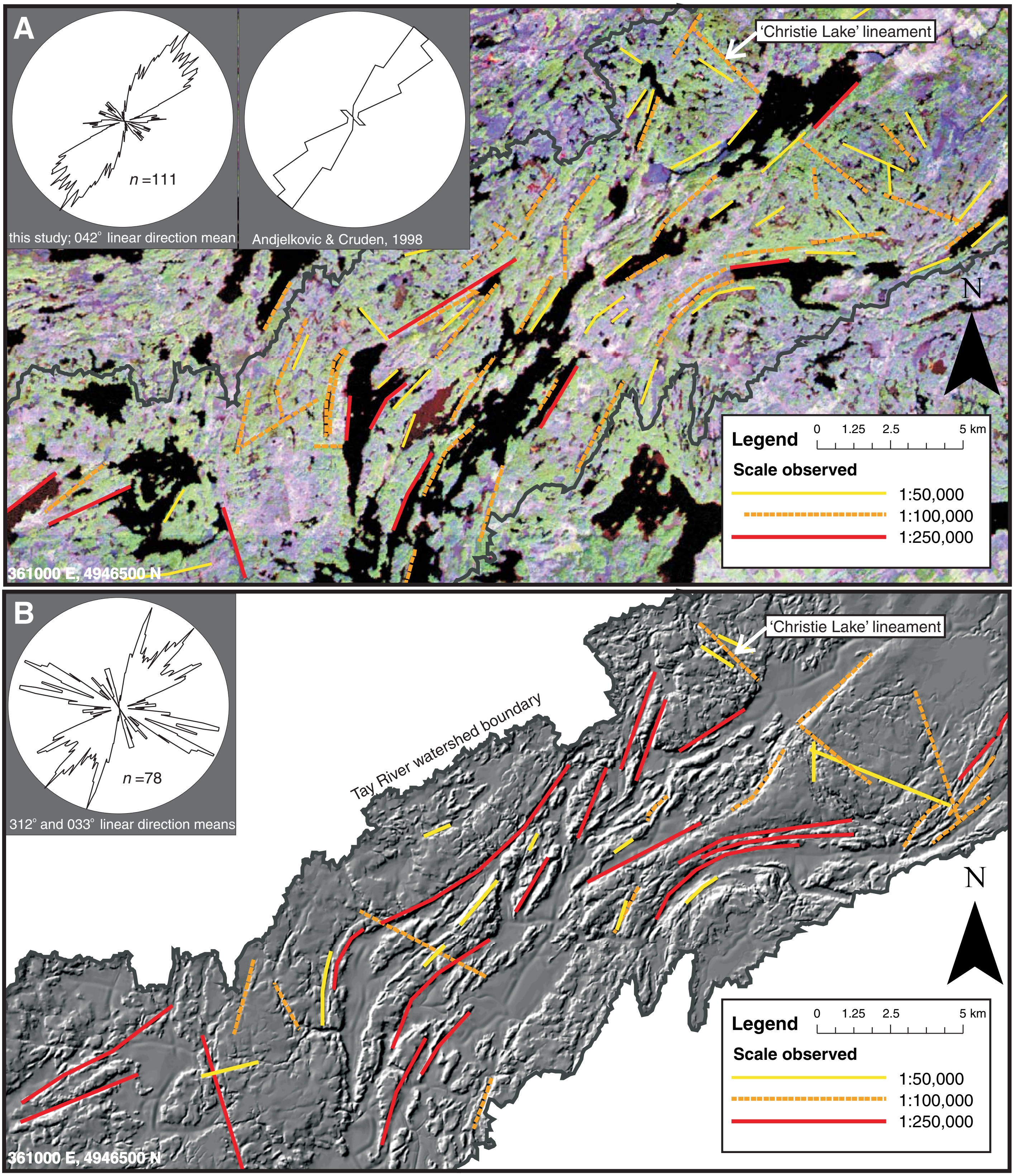

Figure 3. Lineament distributions on (A) Landsat false color composite (bands 754) and (B) hillshade-enhanced digital elevation model (DEM). Both are shown at a scale of 1:100,000, and lineaments are shown by scale of identification. Rose diagrams with 10° bin spacing are inset in each image. Also inset is a rose diagram of lineaments identified by Andjelkovic and Cruden (1998) using Landsat imagery of the Frontenac terrane. The rose diagrams indicate the consistency of identification between different observers and images.

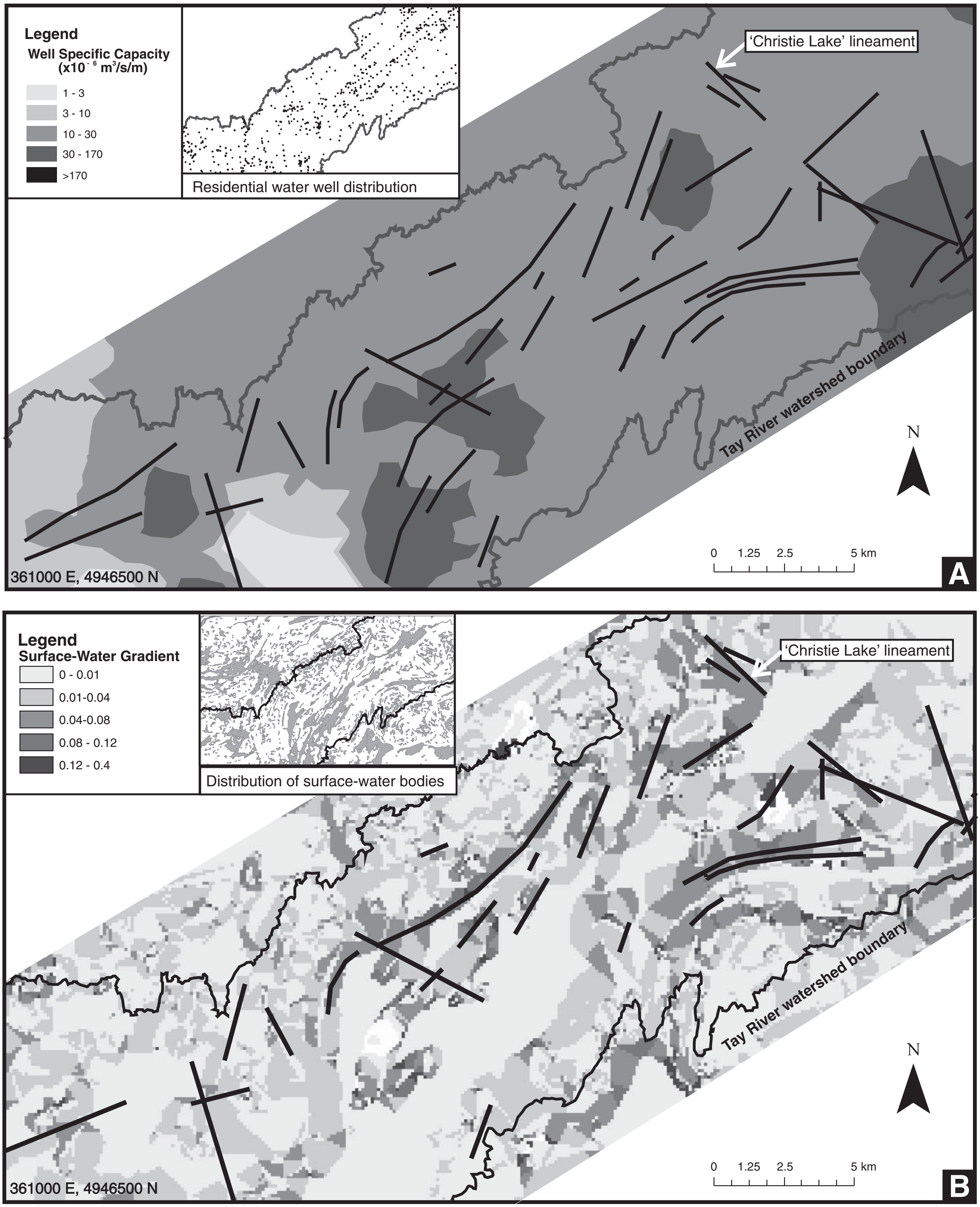

Figure 4. Lineament distribution compared to supplementary geomatic data. (A) Digital elevation model (DEM)–derived lineament distribution compared to residential water well specific capacity. (B) Non–lake shore DEM-derived lineaments compared to interpolated surface-water gradients. Lake shore lineaments are excluded because the surface-water gradient is zero at lake shores by definition. Source data distributions of residential wells (MOE, 2006) and surface-water bodies are shown as insets.

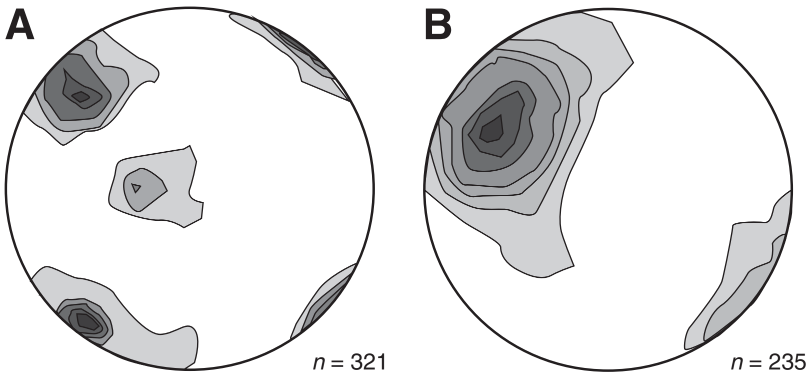

Figure 5. Lower-hemisphere, equal-area stereonets of the poles to (A) fracture and (B) metamorphic foliation measurements from the Tay River watershed, plotted with 2σ uncertainty.

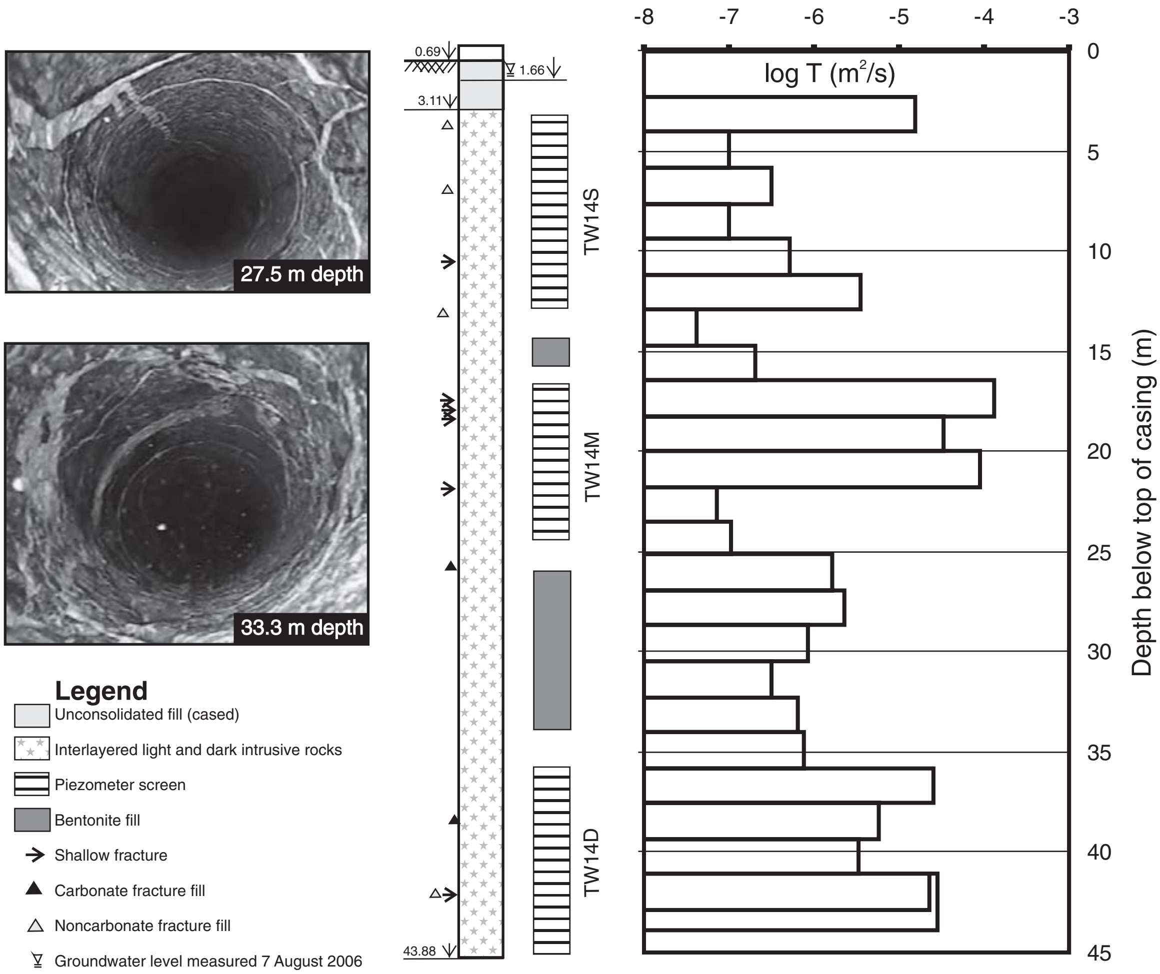

Figure 6. Subsurface data from TW14 borehole drilled in the Christie Lake lineament. Images from downhole camera (borehole diameter is 0.152 m) reveal brecciation and fracture infilling. The presence of carbonate and noncarbonate veins (from chip samples) and horizontal and vertical fractures (from downhole video logging) is noted. Hydraulic testing of 1.77 m test sections was analyzed using the Hvorslev (1951) method. High-transmissivity zones correlate with horizontal fractures observed during video logging. The well was completed with three discrete piezometers (TW14S, TW14M, TW14D) in fractured, transmissive zones.

foliation, which consistently dips moderately to steeply and strikes north-northeast across the watershed (Fig. 5B). The foliation is defined by well-developed schistose and gneissic fabric in metamorphic rocks and poorly to moderately developed schistose and gneissic fabric in plutonic rocks. The least statistically prominent fracture set in outcrop is a shallowly dipping fracture set that is interpreted as sheeting fractures, which are common in crystalline terrains (Sukhija et al., 2006; Novakowski et al., 2007). At the Christie Lake outcrop, the only significant fracture set observed is the steep to vertical northwest set (Fig. 2B).

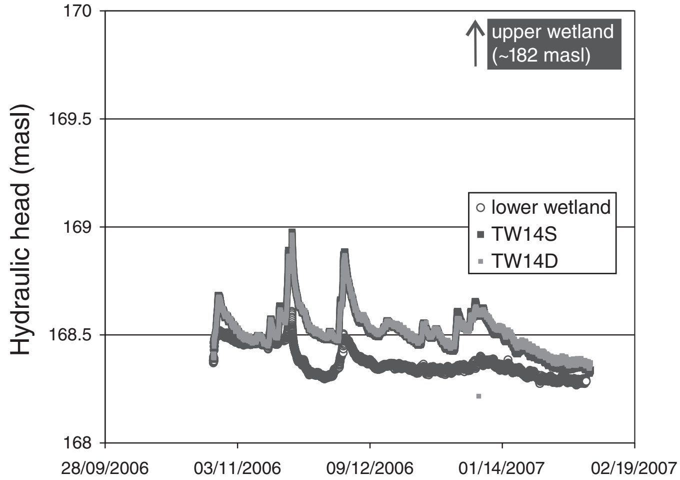

Figure 7. Hydraulic head data from TW14 and the adjacent lower wetland suggest that surface water and groundwater are connected at the Christie Lake lineament (masl—m above sea level).

Hydrogeological Characterization

Subsurface observations from TW14, at the center of the Christie Lake lineament, indicate the presence of both hydraulically significant and insignificant fractures. Qualitative downhole camera observations show pervasive highly angular brecciation and white vein infilling (Fig. 6), which are consistent with previous geological mapping suggesting this lineament is a fault (Wilson, 1961). Brecciation and vein-filling are not in any consistent orientation. Chip samples tested with dilute hydrochloric acid indicate that both carbonate and noncarbonate veins are present. Downhole camera observations also reveal the presence of discrete shallow fractures accentuated by spalling during drilling. The transmissivity distribution indicates that discrete hydraulically significant zones are embedded in generally low-permeability rock (Fig. 6). The low-permeability zones indicate that the pervasive brecciation is not consistently transmissive. Instead, the hydraulically significant zones correlate with the spalled discrete, shallowly dipping fractures (Fig. 6). Therefore, the hydraulically significant zones in this well are assumed to be due to shallowly dipping fracture features, possibly sheeting fractures. The hydraulic conductivity of the shallowly dipping fracture zones is 10^{-3} m/s to 10^{-5} m/s. The effective single-fracture aperture of these fractured zones is 270–540 μm. The lowest hydraulic conductivity intervals (10^{-7} m/s to 2×10^{-8} m/s) are interpreted as the matrix transmissivity, which includes the pervasive infilled veins. Although the matrix may contain numerous small fractures, the extremely limited permeability of these contributes little to the flow system in the fracture network.

Since TW14 is located in a topographic depression with nearby surface-water features at higher elevations, an upward vertical gradient in the well is expected. However, hydraulic head measurements recorded in the piezometers (TW14S, TW14M, and TW14D) indicate that there is effectively no vertical gradient (<0.001) in the well (Fig. 7). The lack of vertical gradient is not due to a short circuit in the well annulus because the well completions were tested and shown to be independent. Water levels in the lower wetland trend with hydraulic head measurements in the shallow and deep piezometers, albeit slightly dampened by the larger storage capacity of the lower wetland. This indicates that the lower wetland and all levels of the well are connected by steeply dipping bedrock fractures. The lack of vertical gradient and correlation in water levels between the lower wetland and piezometers indicate that the subsurface system is connected to the lower wetland but not connected to the upper wetland. The hydraulic testing and water levels also indicate the presence of both shallowly and steeply dipping fractures in the vicinity of TW14. Hydraulic testing results indicate that the shallow fractures are hydraulically significant, but this does not imply a hydraulic significance for the steeply dipping fractures. The hydraulic significance of steeply dipping fractures is explored in the numerical modeling, described in the next section.

The 10 boreholes hand-augured in the lower wetland in a transect perpendicular to the Christie Lake lineament reveal mainly coarse-grained clastics and organics with localized fine-grained material. Each hole was drilled until refusal, which was typically 0.5–2 m depth below ground. The 2.42 m depth of unconsolidated material drilled at TW14 suggests that the depth of refusal is near or at the bedrock interface. The coarse-grained clastics consist of sand and gravel intermixed with modern organic material, consistent with regional-scale descriptions of modern littoral unconsolidated material (Kettles, 1992). A 10-cm-thick layer of clay was found in one borehole, but it has an aerial extent of less than 1 m^2. The predominance of coarse-grained material indicates that there is not extensive overburden with low hydraulic conductivity limiting infiltration at the Christie Lake lineament.

Numerical Simulations of Groundwater–Surface-water Interactions

The model domain is conceptualized in Figure 8A using topography based on a GPS topographic survey of the Christie Lake lineament and subsurface data derived from TW14 hydraulic testing, downhole camera observations, and head measurements (Table 2). The topographic gradient is also consistent with other lineaments in the study area (Fig. 5A). The high topographic gradient and the lack of upward vertical gradient in TW14 suggest that subsurface connectivity is low between the surface-water features. Hydraulic testing data and head data, as well as the fracture sets in the adjacent TG06–07 scan line, indicate the presence of discrete steep and shallow fractures. Unconsolidated material was not considered in the model because the hand-augured boreholes suggest it does not limit infiltration.

Although the hydrogeological characterization of the Christie Lake site clearly indicates the presence of discrete fractures, a preliminary cross-sectional domain was simulated using a porous media approach to constrain the bulk hydraulic conductivity of the system (Fig. 8B). The total transmissivity of TW14 was used as

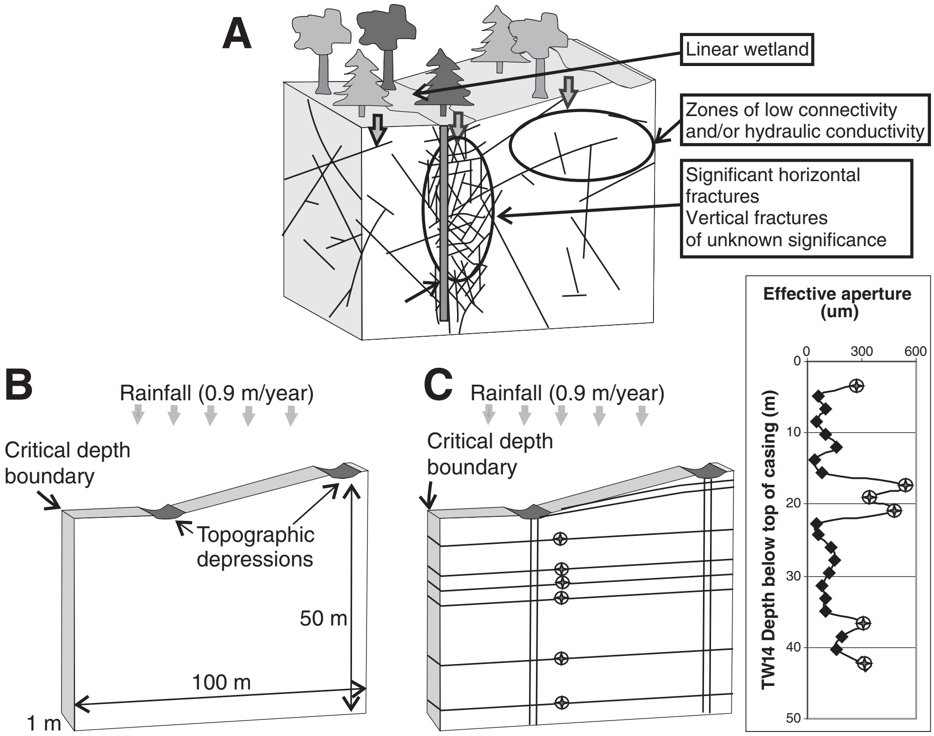

Figure 8. Lineament cross-sectional domain from conceptual model (A) to numerical implementation using an equivalent porous media approach (B) and a discrete fracture network approach (C). Topographic depressions are 2 m deep. The horizontal aperture distribution in the discrete fracture model was derived directly from hydraulic testing of TW14, as described in the text.

TABLE 2. NUMERICAL MODEL INPUT PARAMETERS

Parameter	Value	Unit	Reference
Evapotranspiration			
Evaporation	0.5	m/yr	Golder Associates Ltd. (2003)
Maximum rooting depth	2.0	m	Canadell et al. (1996)
Leaf area index	4	–	Scurlock et al. (2001)
Wilting point	0.06	–	Schroeder et al. (1997)
Field capacity	0.15	–	Schroeder et al. (1997)
Overland flow			
Manning roughness coefficient	0.006	–	Randall (2005)
Rill storage height	0.0001	m	Randall (2005); Therrien et al. (2006)

a starting point, and the hydraulic conductivity was varied using depth of water in the upper wetland as the fitting parameter. The depth of the water in the upper wetland is very sensitive to bulk hydraulic conductivity (Fig. 9A). A range of hydraulic conductivities of less than a half order of magnitude (1.5×10^{-7} to 8×10^{-8} m/s) differentiates dry and overflowing conditions in the upper wetland. The hydraulic conductivities that maintain water in the upper wetland are consistent with measurements interpreted to be the unfractured rock matrix (10^{-7} m/s to 2×10^{-8}m/s), suggesting the area between the two wetlands is largely unfractured. The depth of water in the upper wetland was reproducible to 0.1 m, indicating that the domain is numerically stable and that the depth of water is a useful fitting parameter. The depth of water in the upper wetland was insensitive to evapotranspiration (Fig. 9A).

Subsurface conceptualization and implementation of the discrete fracture network domain was based on hydraulic testing data from TW14 and fracture patterns from TG06–7 (Fig. 2A). An orthogonal fracture network was implemented because vertical and shallowly dipping fractures were observed. Matrix hydraulic conductivity was assigned as the lowest value from hydraulic testing (2×10^{-8} m/s), which is consistent with equivalent porous media model results. Horizontal fracture aperture was assigned directly from hydraulic testing data by calculating a single-fracture effective aperture for each interval (Fig. 8C). The aperture calculation assumes a single fracture is responsible for the measured transmissivity (Fig. 6) of each test interval (Novakowski et al., 2007). Downhole camera data indicate that this was a reasonable assumption because singular fractures can be related to the transmissive zones identified by hydraulic testing. Vertical fractures were assigned to the subsurface below the wetland areas to explore the role of vertical fracture aperture in maintaining a perennial wetland complex with high intervening gradients. The number of vertical fractures underlying each wetland was also varied because the number of vertical fractures is unknown. The depth of the water in the upper wetland is also very sensitive to vertical fracture aperture, with an aperture range of 20 µm differentiating dry and overflowing conditions (Fig. 9B). The maximum vertical fracture aperture that can sustain water in the upper wetland is 60 µm, which is a hydraulically insignificant fracture aperture. Similar to the porous media approach, the depth of water in the upper wetland during discrete fracture network modeling is reproducible and insensitive to evapotranspiration (Fig. 9B). The results from the porous media and discrete fracture network both indicate that low hydraulic conductivity and/or low connectivity are necessary to maintain nearby surface-water bodies with a high intervening gradient.

DISCUSSION

Figure 10 summarizes previous and refined conceptual models for the relationship between lineaments and groundwater flow. In general, lineaments are considered surface expressions of fracture zones, faults, or other subsurface discontinuities (O'Leary et al., 1976; Wise et al., 1985; Singhal and Gupta, 1999). Recent studies have assumed a priori that lineaments are recharge zones with high groundwater potential, which implies high permeability (Fig. 10A; Krishnamurthy et al., 2000; Sener et al., 2005; Shaban et al., 2006). We propose that lineaments in this study area, and likely other geological settings, are surface expressions of structural features with diminished permeability due to structural and/or fluid flow processes (Fig. 10B).

A myriad of structural and tectonic processes has been proposed for the origin of lineaments (Wise et al., 1985). The different structural processes can be categorized simplistically into those with displacement (faults) and those without displacement. Defining a kinematic and dynamic structural model for the development of lineaments in this study area is impossible due to the poor exposure of lineaments. Instead, we compile fracture patterns and geologic data to define possible structural styles of lineaments. The coincidence of fracture orientations and lineament orientations both at a regional scale and at the Christie Lake study area suggests that lineaments are structurally controlled (Figs. 2, 3, and 5). The predominant lineament set trends northeast with a linear direction mean orientation of 042° (Landsat) or 033° (DEM). The northeast-trending lineament set parallels the steep, northeast-striking fracture set (Fig. 5A) and the regional structural grain defined in outcrop by schistose and gneissic foliation (Fig. 5B). The northeast-trending fracture and lineament set is not consistent with any recognized regional brittle fault structures. The major northeast-striking structures are ductile shear zones (Easton, 1992; Davidson and Ketchum, 1993). The northeastern lineaments are likely a result of minimal displacement in zones of joints developed parallel to the well-developed metamorphic grain (Andjelkovic and Cruden, 1998). An alternative explanation is that the northeast-trending lineament set may be due to glacial landforms, since southwest-northeast is the direction of glacial advance and retreat (Kettles, 1992). However, the northeastern lineaments are not likely of glacial origin because the discontinuous till veneer rarely masks the structure of the underlying bedrock (Kettles, 1992).

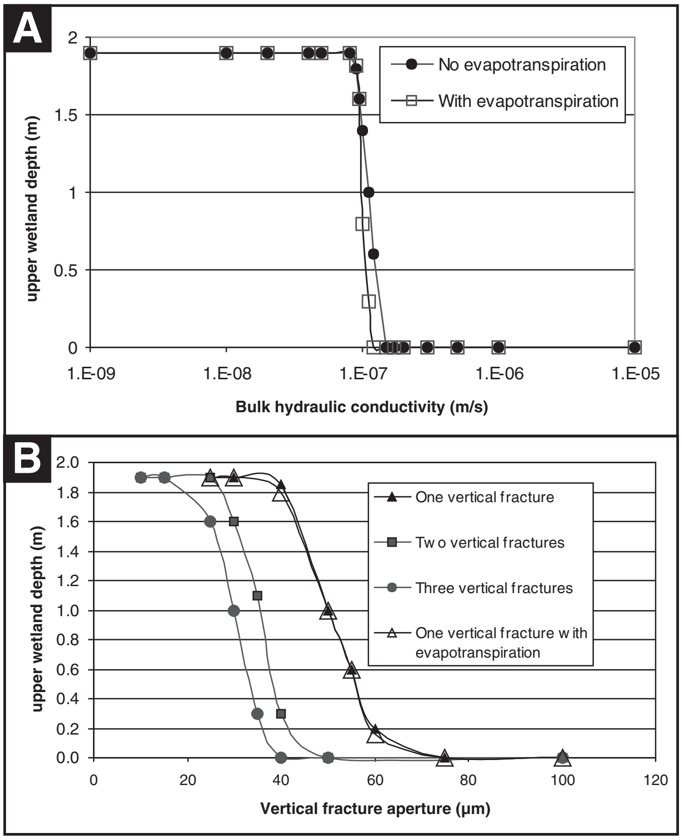

Figure 9. Numerical model results for lineament cross-sectional domain showing depth of water in the upper wetland with varying bulk hydraulic conductivity using an equivalent porous media approach (A) and vertical fracture aperture using a discrete fracture network approach (B). A very limited range of hydraulic conductivities or fracture apertures maintains the depth of water in the upper wetland without overflowing it, suggesting that subsurface permeability controls the distribution of perennial surface-water features. The similarity of results incorporating evapotranspiration indicates that evapotranspiration is not an important control on the depth of water in surface-water bodies.

The secondary northwest-trending lineament set with a linear directional mean of 312° was observed in the DEM data but not in Landsat imagery in this study and a previous study (Andjelkovic and Cruden, 1998). The northwest-trending lineament set parallels the vertical northwest-striking fracture set (Fig. 5A). The Christie Lake lineament is part of this lineament set and is interpreted as a fault based on the subsurface brecciation (Fig. 6), the linear topographic break (Fig. 2), and the mapped unit truncation to the northwest (Wilson, 1961). Permeability reduction at the Christie Lake lineament is discussed later. The north-facing topographic break, the northwest lineament trend, and the vertical northwest-striking fracture set suggest that the faulted Christie Lake lineament is part of the Ottawa-Bonnechere graben system (Kumarapeli, 1978; Rimando and Benn, 2005). Northwest-trending lineaments in eastern Ontario, which decrease in frequency away from the center of the graben, have been previously interpreted as part of the Ottawa-Bonnechere graben (Spitzer, 1981). The interpretation of the Christie Lake lineament as a fault associated with the Ottawa-Bonnechere graben suggests that other northwest-trending lineaments may also be associated with faults. Northwest-trending lineaments were not observed in Landsat imagery, suggesting that digital elevation models (or other topographic remote imagery) may be more useful for identifying faults at a regional scale than tonal remote imagery, especially in topographically subdued terrain (Nyborg et al., 2007).

Previous studies document limited or inconsistent correlation between well yields and lineaments, suggesting that the permeability underlying lineaments is variable (Waters et al., 1990; Gustafsson, 1994; Mabee et al., 1994; Sander et al., 1997; Edet et al., 1998; Mabee, 1999; Magowe and Carr, 1999; Moore et al., 2002). Similarly, permeable zones with high inflow in bedrock tunnels do not correlate consistently with the location of lineaments (Banks et al., 1992; Mabee et al., 2002). The lack of correlation can be attributed to the presence of shallow-dipping sheeting fractures, which are not detected during lineament analysis (Mabee et al., 2002), or the presence of fault cores (Banks et al., 1992). Well yields in this study area are actually lower in areas near lineaments (Table 1). Lower well yields in conjunction with high surface-water gradient (Fig. 4B) suggest that lineaments in this study are potential hydraulic barriers with low to moderate permeability and connectivity. The similarity in orientation, length, topography (Fig. 3B), surface-water gradient (Fig. 4B) and specific capacity (Fig. 4A) of the Christie Lake site to other areas in this study suggest that the Christie Lake lineament is a representative lineament. Therefore, the conclusions based on the

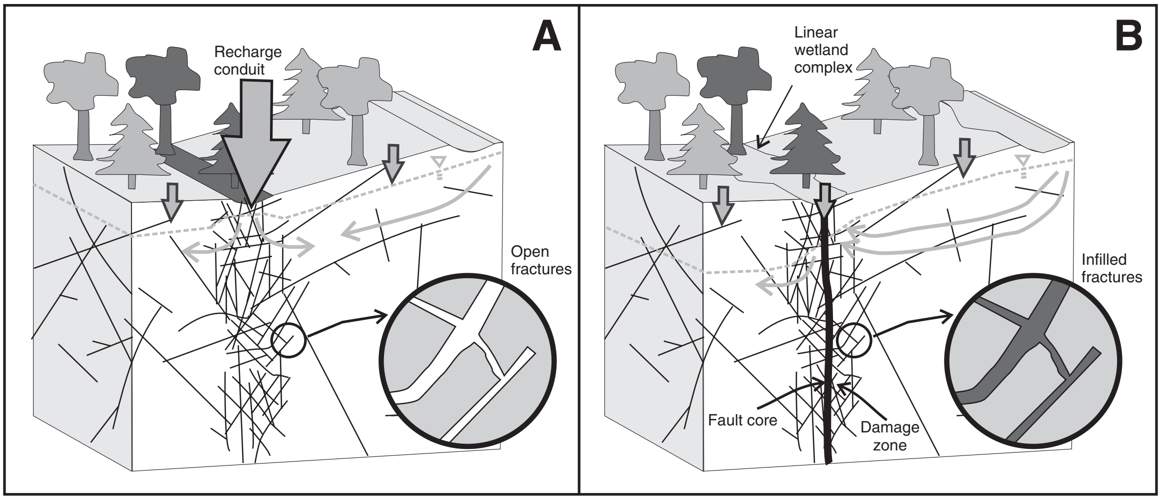

Figure 10. An idealized cross-sectional domain showing (A) previous and (B) new conceptual models of the relationship between lineaments and groundwater. The surface expression of the lineament is a topographic depression and a tonal difference, highlighted here by the dark trees. Below the surface, lineaments are generally considered to be zones of intense fractures and joints. Approximate flow lines are shown, but true flow paths would depend on the connectivity and aperture distribution of the fracture network. Recent recharge studies have assumed lineaments have a higher groundwater potential due to the intense fracturing. Contrary to previous studies, lineaments in this study are surface-water features with low permeability and/or connectivity due to structural and/or fluid flow processes.

hydrogeological characterization and numerical experiments have implications for other lineaments. Subsurface permeability of the Christie Lake lineament is controlled by discrete shallow and steep fractures. Numerical modeling indicates that the steep fractures must have small apertures to maintain adjacent surface-water features with high intervening gradients. Therefore, lineaments in this study area are likely zones where limited or diminished fracture aperture, density, or connectivity results in low-permeability barriers to flow.

The reduction of permeability is likely the result of fault core development and/or mineral deposition during or after faulting. Permeability is reduced in fault cores due to brecciation, cataclasis, the development of clay-rich gouge zones, and other processes reviewed by Caine et al. (1996). Low-permeability, clay-rich fault features have been observed directly below lineaments in a bedrock tunnel through Precambrian granite (Banks et al., 1992). Numerous drilling records near lineaments in the study area record "granite" overlying "clay," which is consistent with fault core development in a crystalline setting. The reduced permeability of the Christie Lake lineament, which is interpreted as a fault, may be due to fault core development, even though a fault core was not observed in TW14. TW14 is interpreted to have drilled through the damage zone of the Christie Lake lineament-fault based on the pervasive brecciation and vein-infilling. The location of the potential fault core, the size of the damage zone, and other fault architecture characteristics (Caine et al., 1996) cannot be quantified due the lack of exposed lineament outcrop. Permeability can also be reduced by syn- or postdeformation fluids infilling fractures by depositing dissolved constituents (Evans and Chester, 1995; Goddard and Evans, 1995). Pervasive fracture infilling is evidenced in downhole video camera data from TW14. Chip samples recovered during drilling suggest that both carbonate and noncarbonate minerals are infilling fractures. The infilled brecciation suggests that the examined area of the Christie Lake lineament-fault was previously a fluid conduit but that fault and fluid flow processes together led to permeability reduction. Therefore, the reduction of permeability associated with lineaments in the study area is probably a result of fault characteristics common in crystalline settings: clay-rich fault cores and damage zones that are heavily fractured and vein-infilled.

Reduced fault-zone permeability can compartmentalize regional groundwater flow (Ferrill et al., 2004). High surface-water gradients (Fig. 4B), hung wetland complexes upgradient of the Christie Lake lineament and other lineaments, numerical modeling results (Fig. 9), and the subsurface conceptual model (Fig. 10B) suggest that lineaments in this study area are barriers that are compartmentalizing flow. Detailed fault studies in other regions suggest that fault architecture is extremely complex and heterogeneous (Evans and Chester, 1995; Caine and Forster, 1999; Fairley and Hinds, 2004; Minor and Hudson, 2006), so the permeability reduction may or may not be persistent along strike over kilometers. Numerical modeling and field examples discussed by Bense and Person (2006) indicate that faults with large hydraulic head discontinuities can be conduit-barrier systems with significant preferential flow parallel to the fault, rather than pure hydraulic barriers. However, the pervasive fracture infilling observed in TW14, measured low hydraulic conductivity in the damage zone, and ubiquitous surface-water bodies along lineaments suggest that significant preferential flow and recharge along the Christie Lake lineament and other lineaments is not likely.

CONCLUSIONS AND IMPLICATIONS

We investigated lineaments as geological structures that could impact regional flow systems in a low-gradient crystalline bedrock aquifer in the Canadian Shield. We identified and characterized watershed-scale low-permeability zones by integrating diverse geomatic, geological, and hydrogeological data sets and numerical simulations. Salient conclusions from this study area include: (1) lineaments are structural features, either fault zones or fracture zones with limited displacement; (2) the fractured bedrock underlying lineaments is composed of poorly connected, low-permeability zones due to fault zone and/or fluid flow processes; (3) permeability reduction results in lineament areas being recharge and flow barriers that compartmentalize lateral flow systems; and (4) faulted lineaments can be more effectively identified by topographic data (e.g., DEM) than by tonal imagery (e.g., Landsat). Although lineaments have been controversial in the geological and hydrogeological literature, this study shows that lineaments are important and useful if identified with a defensible method and analyzed with supplementary geomatic, geologic, and hydrogeologic data within a well-documented structural geology framework.

The interpretation of lineaments as watershed-scale, low-permeability zones in this study area may affect recharge estimates and contaminant disposal practices in crystalline settings. Recharge estimates are critical for determining groundwater sustainability in water resource management. Recharge in crystalline bedrock aquifers is considered very limited (Rodhe and Bockgard, 2006; Milloy, 2007). Recent studies applying remote sensing and geospatial analysis have assumed a priori that lineaments are recharge zones (Krishnamurthy et al., 2000; Sener et al., 2005; Shaban et al., 2006). However, if lineaments are low-permeability structures, the recharge potential of lineaments may be quite limited, and thus assuming that lineaments are recharge zones would be misleading in this study area. Various northern countries plan to dispose of nuclear waste in saturated crystalline repositories. Quantification of the permeability of lineaments and other geological structures is a significant concern when modeling the time of travel for nuclide transport to the biosphere.

This study shows that diverse data sets and geologically realistic models of lineament permeability are necessary to unravel patterns of fluid flow in the brittle uppermost crust (<100 m depth). The relationship between permeability and fault architecture was originally documented at the outcrop scale or site scale (Evans and Chester, 1995; Caine et al., 1996; Evans et al., 1997; Schulz and Evans, 2000; Rawling et al., 2001). Results from this study support other recent studies suggesting that brittle structures control regional groundwater flow in bedrock aquifers and that fault architecture models are a useful framework for examining the permeability of regional structures (Ferrill et al., 2004; Seaton and Burbey, 2005; Bense and Person, 2006; Denny et al., 2007). Although the study area is located in a Precambrian shield where deformation is ancient and polyphased, fault architecture and permeability studies suggest that these results may be applicable to other areas with different protoliths or where deformation is more recent and less complex (Evans, 1988; Caine et al., 1996; Caine and Forster, 1999; Rawling et al., 2001).

APPENDIX

Multiple data types highlight different lineament characteristics resulting in a defensible lineament identification method (Mabee et al., 1994; Clark et al., 1996; Sander et al., 1997). Landsat imagery highlights tonal differences; a digital elevation model (DEM) reveals topographic differences; and aerial photographs show detailed geomorphology. To conduct this study, a multispectral Landsat 5 Thematic Mapper image with 30 m resolution was acquired at 15:34:50 on 26 September 2004 from orbit 109424. The center of the frame is 44.61°N. False color composites of bands 742, 754, and 432 were examined, but false color composite 754 was the most useful, as found by Andjelkovic and Cruden (1998). The DEM was developed by the Ontario Ministry of Natural Resources and is accurate to ±5 m vertically and ±10 m horizontally, with a raster resolution of 10 m. Surface-water elevations are considered representative at ±5 m because elevations were corrected to provincial time-series flow data. For lineament identification, the DEM was hillshade-enhanced to accentuate features in the subdued landscape. Aerial photographs of selected areas at 1:5000 to 1:12,000 scales were examined to further characterize the geomorphology and hydrology of lineaments during ground truthing.

Lineaments were identified on DEM and the false color composite Landsat images at scales of 1:250,000, 1:100,000, and 1:50,000. The scales observed are considered an important lineament characteristic for classifying the spatial significance of the lineament. Lineament attributes (azimuth, scale observed, date observed, and curvilinear form) were compiled during identification. All lineaments were identified manually because attempts at automated lineament detection primarily identified anthropomorphic features. Lineaments were observed during multiple trials separated by a week to test reproducibility (Mabee et al., 1994). All lineaments not repeatedly identified at the same scale, as well as all anthropomorphic lineaments (roads, electrical lines, etc.), were removed from the database. In addition, lineaments derived from Landsat imagery were compared to lineaments derived from the same area using a different Landsat image by Andjelkovic and Cruden (1998; Fig. 3). Lineaments were not explicitly correlated to nearby fracture patterns, as recommended by Mabee et al. (1994), in order to keep the lineament and fracture databases independent for subsequent structural analysis. Lineament orientation was plotted as rose diagrams with a 10° smoothing function, and the linear directional mean was calculated.

ACKNOWLEDGMENTS

This research was funded by the Ontario Research and Development Fund, Natural Science and Engineering Research Council of Canada and the Rideau Valley Conservation Authority. D. Andjelkovic, S. Cruden, L. Godin, R. Harrap, J. Kozuskanich, R. McLaren, T. Praamsma, K. Raven, and R. Zavitz contributed advice on or editing for earlier versions of the manuscript. Dong Mei Chen generously provided Landsat imagery. Stereonets and rose diagrams were plotted with *Stereonet* by R. Allmendinger and *LDIS* by E. Erslev, respectively. Imagery enhancement and geomatic analysis were completed in PCI Geomatica and ARC GIS 9.0, respectively. Reviews and comments by V. Bense, F. Day-Lewis, Associate Editor M. Person, and Editor K. Karlstrom greatly improved the manuscript.

REFERENCES CITED

American Society for Testing and Materials, 2007, Bailey, S.J., et al., eds., Classification of Soils for Engineering Purposes: Annual Book of ASTM Standards, D2487–83, v. 04–08, p. 395–408.

Andjelkovic, D., and Cruden, A.R., 1998, Relationships between fractures in Paleozoic cover rocks and structures in the Precambrian basement, south-central Ontario, *in* Summary of Fieldwork and Other Activities 1998: Ontario Geological Survey Miscellaneous Paper 169, p. 275–280.

Banks, D., Solbjorg, M.L., and Rohr-Torp, E., 1992, Permeability of fracture zones in a Precambrian granite: Quarterly Journal of Engineering Geology, v. 25, p. 377–388, doi: 10.1144/GSL.QJEG.1992.025.04.12.

Becker, M.W., 2006, Potential for satellite remote sensing of ground water: Ground Water, v. 44, no. 2, p. 306–318, doi: 10.1111/j.1745-6584.2005.00123.x.

Bense, V.F., and Person, M.A., 2006, Faults as conduit-barrier systems to fluid flow in siliciclastic sedimentary aquifers: Water Resources Research, v. 42, p. doi: 10.1029/2005WR004480.

Berkowitz, B., 2002, Characterizing flow and transport in fractured geological media: A review: Advances in Water Resources, v. 25, p. 861–884, doi: 10.1016/S0309-1708(02)00042-8.

Brunner, P., Franssen, H.J.H., Kgotlhang, L., Bauer-Gottwein, P., and Kinzelbach, W., 2007, How can remote sensing contribute in groundwater modeling?: Hydrogeology Journal, v. 15, no. 1, p. 5–18, doi: 10.1007/s10040-006-0127-z.

Butler, J.J., Jr., 1998, The Design, Performance and Analysis of Slug Tests: Boca Raton, Florida, CRC Press, 245 p.

Caine, J.S., and Forster, C.B., 1999, Fault zone architecture and fluid flow: Insights from field data and numerical modeling, *in* Haneberg, W.C., Mozley, P.S., Moore, J.C., and Goodwin, L.B., eds., Faults and subsurface fluid flow in the shallow crust: American Geophysical Union Geophysical Monograph 113, p. 101–127.

Caine, J.S., and Tomusiak, S.R.A., 2003, Brittle structures and their role in controlling porosity and permeability in a complex Precambrian crystalline-rock aquifer system in the Colorado Rocky Mountain Front Range: Geological Society of America Bulletin, v. 115, no. 11, p. 1410–1424, doi: 10.1130/B25088.1.

Caine, J.S., Evans, J.P., and Forster, C.B., 1996, Fault zone architecture and permeability structure: Geology, v. 24, no. 11, p. 1025–1028, doi: 10.1130/0091-7613(1996)024<1025:FZAAPS>2.3.CO;2.

Canadell, J., Jackson, R.B., Ehleringer, J.R., Mooney, H.A., Sala, O.E., and Schulze, E.D., 1996, Maximum rooting depth of vegetation types at the global scale: Oecologia, v. 108, no. 4, p. 583–595, doi: 10.1007/BF00329030.

Cey, E., Rudolph, D., and Therrien, R., 2006, Simulation of groundwater recharge dynamics in partially saturated fractured soils incorporating spatially variable fracture apertures: Water Resources Research, v. 42, p. doi: 10.1029/2005WR004589.

Chester, F.M., Evans, J.P., and Biegel, R.L., 1993, Internal structure and weakening mechanisms of the San Andreas fault: Journal of Geophysical Research, v. 98, p. 771–786, doi: 10.1029/92JB01866.

Clark, S.F., Jr., Moore, R.B., Ferguson, E.W., and Picard, M.Z., 1996, Criteria and Methods for Fracture-Trace Analysis of the New Hampshire Bedrock Aquifer: U.S. Geological Survey Open-File Report 96–479, 12 p.

Culotta, R.C., Pratt, T., and Oliver, P.J., 1990, A tale of two sutures: COCORP's deep seismic surveys of the Grenville province in the eastern U.S. Midcontinent: Geology, v. 18, p. 646–649, doi: 10.1130/0091-7613(1990)018<0646:ATOTSC>2.3.CO;2.

Davidson, A., and Ketchum, J.W.F., 1993, Observations of the Maberly shear zone, a terrane boundary within the Central Metasedimentary Belt, Grenville Province, Ontario: Geological Survey of Canada, Current Research Paper 93–1C, p. 265–269.

Denny, S.C., Allen, D.M., and Journeay, J.M., 2007, DRASTIC-Fm: A modified vulnerability mapping method for structurally controlled aquifers in the southern Gulf Islands, British Columbia, Canada: Hydrogeology Journal, v. 15, p. 483–493, doi: 10.1007/s10040-006-0102-8.
Easton, R.M., 1992, The Grenville Province, *in* Thurston, P.C., Williams, H.R., Sutcliffe, R.H., and Stott, G.M., eds., Geology of Ontario: Ottawa, Ontario Geological Survey, Special Volume 4, Part 2, p. 713–904.
Easton, R.M., 2001, Precambrian Geology, Tichborne Area: Ontario Geological Survey Map P-3442, scale 1:50,000.
Edet, A.E., Okereke, C.S., Teme, S.C., and Esu, E.O., 1998, Application of remote-sensing data to groundwater exploration: A case study of the Cross River State, southeastern Nigeria: Hydrogeology Journal, v. 6, p. 394–404, doi: 10.1007/s100400050162.
Evans, J.P., 1988, Deformation mechanisms in granitic rocks at shallow crustal levels: Journal of Structural Geology, v. 10, p. 437–443, doi: 10.1016/0191-8141(88)90031-4.
Evans, J.P., and Chester, F.M., 1995, Fluid-rock interaction in faults of the San Andres system: Inferences from San Gabriel fault rock geochemistry and microstructures: Journal of Geophysical Research, v. 100, p. 13,007–13,020, doi: 10.1029/94JB02625.
Evans, J.P., Forster, C.B., and Goddard, J.V., 1997, Permeability of fault-related rocks, and the implications for hydraulic structure of fault zones: Journal of Structural Geology, v. 19, p. 1393–1404, doi: 10.1016/S0191-8141(97)00057-6.
Fairley, J.P., and Hinds, J.J., 2004, Rapid transport pathways for geothermal fluids in an active Great Basin fault zone: Geology, v. 32, no. 9, p. 825–828, doi: 10.1130/G20617.1.
Farvolden, R.N., Pfannkuch, O., Pearson, R., and Fritz, P., 1988, Region 12, Precambrian Shield, *in* Back, W., Rosenshein, J.S., and Seaber, P.R., eds., Hydrogeology: Boulder, Colorado, Geological Society of America, The Geology of North America, v. O-2, p. 101–114.
Ferrill, D.A., Sims, D.W., Waiting, D.J., Morris, A.P., Franklin, N.M., and Schultz, A.L., 2004, Structural framework of the Edwards Aquifer recharge zone in south-central Texas: Geological Society of America Bulletin, v. 116, p. 407–418, doi: 10.1130/B25174.1.
Flint, A.L., Flint, L.E., Kwicklis, E.M., Bodvarsson, G.S., and Fabryka-Martin, J.M., 2001, Hydrology of Yucca Mountain: Reviews of Geophysics, v. 39, no. 4, p. 447–470, doi: 10.1029/1999RG000075.
Flint, A.L., Flint, L.E., Kwicklis, E.M., Fabryka-Martin, J.M., and Bodvarsson, G.S., 2002, Estimating recharge at Yucca Mountain, Nevada, USA: Comparison of methods: Hydrogeology Journal, v. 10, p. 180–204, doi: 10.1007/s10040-001-0169-1.
Forster, C.B., and Evans, J.P., 1991, Hydrogeology of thrust faults and crystalline thrust sheets: Results from combined field and modeling studies: Geophysical Research Letters, v. 18, p. 979–982, doi: 10.1029/91GL00950.
Fredrick, K.C., Becker, M.W., Matott, L.S., Daw, A., Bandilla, K., and Flewelling, D.M., 2007, Development of a numerical groundwater flow model using SRTM elevations: Hydrogeology Journal, v. 15, no. 1, p. 171–181, doi: 10.1007/s10040-006-0115-3.
Freeze, R.A., and Cherry, J.A., 1979, Groundwater: Eaglewood Cliffs, New Jersey, Prentice-Hall Inc., 604 p.
Goddard, J.V., and Evans, J.P., 1995, Chemical changes and fluid-rock interaction in faults of crystalline thrust sheets, northwestern Wyoming, U.S.A.: Journal of Structural Geology, v. 12, p. 869–882.
Golder Associates Ltd., 2003, Renfrew County-Mississippi-Rideau Groundwater Study: Ottawa, Ontario, 32 p.
Gustafsson, P., 1994, SPOT satellite data for exploration of fractured aquifers in a semi-arid area in southeastern Botswana: Applied Hydrogeology, v. 2, p. 9–18, doi: 10.1007/s100400050246.
Hvorslev, M.J., 1951, Time Lag and Soil Permeability in Ground-Water Observations: U.S. Army Corps of Engineers Waterways Experimental Station Bulletin 36, 50 p.
Isachsen, Y.W., 1976, Fracture analysis of New York State using multi-stage remote sensing data and ground study; possible application to plate tectonic modeling, *in* Hodgson, R.A., Gay, S.P., Jr., and Benjamins, J.Y., eds., Proceedings of the First International Conference on the New Basement Tectonics: Utah Geological Association Publication 5, p. 200–217.
Jackson, J.A., ed., 1997, Glossary of Geology: Alexandria, Virginia, American Geological Institute, 769 p.
Kay, G.M., 1942, Ottawa-Bonnechere graben and Lake Ontario homocline: Geological Society of America Bulletin, v. 53, p. 585–646.
Kettles, I.M., 1992, Glacial Geology and Glacial Sediment Geochemistry in the Clyde Forks–Westport Area of Ontario: Geological Survey of Canada Paper 92-17, 34 p.
Krishnamurthy, J., Mani, A., Jayaraman, V., and Manivel, M., 2000, Groundwater resources development in hard rock terrain—An approach using remote sensing and GIS techniques: International Journal of Applied Earth Observation and Geoinformation, v. 2, no. 3–4, p. 204–215, doi: 10.1016/S0303-2434(00)85015-1.
Kumarapeli, P.S., 1978, The St. Lawrence paleo-rift system: A comparative study, *in* Ramberg, I.B., and Neumann, E.R., eds., Tectonics and Geophysics of Continental Rifts: Dordrecht, Netherlands, D. Reidel Publishing, p. 367–384.
Kumarapeli, P.S., 1981, Origin and development of the Ottawa graben, *in* Conference on Processes of Planetary Rifting Abstracts: Houston, Lunar and Planetary Institute, p. 114–116.
La Pointe, P.R., and Hudson, J.A., 1985, Characterization and Interpretation of Rock Mass Joint Patterns: Geological Society of America Special Paper 199, 37 p.
Lattman, L.H., and Matzke, R.H., 1971, Fracture traces and joints in central Pennsylvania: American Association of Petroleum Geologists Bulletin, v. 55, no. 10, p. 1878–1881.
Lattman, L.H., and Parizek, R.R., 1964, Relationship between fracture traces and the occurrence of groundwater in carbonate rocks: Journal of Hydrology, v. 2, p. 73–91, doi: 10.1016/0022-1694(64)90019-8.
Mabee, S.B., 1999, Factors influencing well productivities in glaciated metamorphic rocks: Ground Water, v. 37, p. 88–97, doi: 10.1111/j.1745-6584.1999.tb00961.x.
Mabee, S.B., Hardcastle, K.C., and Wise, D.U., 1994, A method of collecting and analyzing lineaments for regional-scale fractured-bedrock aquifer studies: Ground Water, v. 32, no. 6, p. 884–894, doi: 10.1111/j.1745-6584.1994.tb00928.x.
Mabee, S.B., Curry, P.J., and Hardcastle, K.C., 2002, Correlation of lineaments to ground water inflows in a bedrock tunnel: Ground Water, v. 40, no. 1, p. 37–43, doi: 10.1111/j.1745-6584.2002.tb02489.x.
Magowe, M., and Carr, J.R., 1999, Relationship between lineaments and ground water occurrence in western Botswana: Ground Water, v. 37, no. 2, p. 282–286, doi: 10.1111/j.1745-6584.1999.tb00985.x.
Marler, J., and Ge, S., 2003, The permeability of the Elkhorn fault zone, South Park: Colorado: Ground Water, v. 41, no. 3, p. 321–332, doi: 10.1111/j.1745-6584.2003.tb02601.x.
Mayer, J.R., and Sharp, J.M., 1998, Fracture control of regional ground-water flow in a carbonate aquifer in a semi-arid region: Geological Society of America Bulletin, v. 110, no. 2, p. 269–283, doi: 10.1130/0016-7606(1998)110<0269:FCORGW>2.3.CO;2.
Milloy, C.A., 2007, Measurement of Hydraulic Head for the Evaluation of Groundwater Recharge to Discrete Fracture Zones in a Crystalline Bedrock Aquifer [M.Sc. thesis]: Kingston, Ontario, Queen's University, 131 p.
Minor, S.A., and Hudson, M.R., 2006, Regional survey of structural properties and cementation patterns of fault zones in the northern part of the Albuquerque Basin, New Mexico: Implications for ground-water flow: U.S. Geological Survey Professional Paper 1719, 34 p.
MOE (Ministry of the Environment), 2006, Water Well Information System Database: Toronto, Ontario, Ontario Ministry of the Environment.
Moore, R.B., Schwarz, G.E., Clark, S.F., Jr., Walsh, G.J., and Degnan, J.R., 2002, Factors Related to Well Yield in the Fractured-Bedrock Aquifer of New Hampshire: U.S. Geological Survey Professional Paper 1660, 51 p.
Novakowski, K.S., Lapcevic, P.A., and Sudicky, E.A., 2007, Groundwater flow and solute transport in fractured media, *in* Delleur, J.W., ed., Handbook of Groundwater Engineering: Boca Raton, Florida, CRC Press, p. 20-1–20-43.
Nyborg, M., Berglund, J., and Triumf, C.-A., 2007, Detection of lineaments using airborne laser scanning technology: Laxemar-Simpevarp, Sweden: Hydrogeology Journal, v. 15, no. 1, p. 29–32, doi: 10.1007/s10040-006-0134-0.
O'Leary, D.W., Friedman, J.D., and Pohn, H.A., 1976, Lineament, linear, lineation: Some proposed new standards for old terms: Geological Society of America Bulletin, v. 87, p. 1463–1469, doi: 10.1130/0016-7606(1976)87<1463:LLLSPN>2.0.CO;2.
Panday, S., and Huyakorn, P.S., 2004, A fully coupled physically-based spatially-distributed model for evaluating surface/subsurface flow: Advances in Water Resources, v. 27, no. 4, p. 361–382, doi: 10.1016/j.advwatres.2004.02.016.
Praamsma, T.W., 2006, Complex Groundwater–Surface Water Interaction in a Gneissic Terrain [M.Sc. thesis]: Kingston, Ontario, Queen's University, 115 p.
Prost, G.L., 1994, Remote Sensing for Geologists: A Guide to Image Interpretation: Amsterdam, Gordon and Breach Science, 326 p.
Randall, J.E., 2005, The Analysis of Seasonally Varying Flow in a Crystalline Rock Watershed Using an Integrated Surface Water and Groundwater Model [M.Sc. thesis]: Waterloo, Ontario, University of Waterloo, 88 p.
Rawling, G.C., Goodwin, L.B., and Wilson, J.L., 2001, Internal architecture, permeability and hydrologic significance of contrasting fault-zone types: Geology, v. 29, no. 1, p. 43–46, doi: 10.1130/0091-7613(2001)029<0043:IAPSAH>2.0.CO;2.
Rimando, R.E., and Benn, K., 2005, Evolution of faulting and paleo-stress field within the Ottawa graben, Canada: Journal of Geodynamics, v. 39, no. 4, p. 337–360, doi: 10.1016/j.jog.2005.01.003.
Rodhe, A., and Bockgard, N., 2006, Groundwater recharge in a hard rock aquifer: A conceptual model including surface-loading effects: Journal of Hydrology, v. 330, p. 389–401, doi: 10.1016/j.jhydrol.2006.03.032.
Sander, P., 2007, Lineaments in groundwater exploration: A review of applications and limitations: Hydrogeology Journal, v. 15, no. 1, p. 71–74, doi: 10.1007/s10040-006-0138-9.
Sander, P., Minor, T.B., and Chesley, M.M., 1997, Groundwater exploration based on lineament analysis and reproducibility tests: Ground Water, v. 35, no. 5, p. 888–894, doi: 10.1111/j.1745-6584.1997.tb00157.x.
Schroeder, P.R., Dozier, T.S., Zappi, P.A., McEnroe, B.M., Sjostrom, J.W., and Payton, R.L., 1997, The Hydrologic Evaluation of Landfill Performance (HELP) Model, Engineering Documentation for Version 3: Vicksburg, Mississippi, U.S. Army Corps of Engineers, 84 p.
Schulz, S.E., and Evans, J.P., 2000, Mesoscopic structure of Punchbowl fault, Southern California and the geological and geophysical structure of active strike-slip faults: Journal of Structural Geology, v. 22, p. 913–930, doi: 10.1016/S0191-8141(00)00019-5.
Scurlock, J.M.O., Asner, G.P., and Gower, S.T., 2001, Worldwide Historical Estimates and Bibliography of Leaf Area Index, 1932–2000: Oak Ridge National Laboratory Technical Memorandum TM-2001/268, 40 p.
Seaton, W.J., and Burbey, T.J., 2005, Influence of ancient thrust faults on the hydrogeology of the Blue Ridge Province: Ground Water, v. 43, no. 3, p. 301–313, doi: 10.1111/j.1745-6584.2005.0026.x.
Sener, E., Davraz, A., and Ozcelik, M., 2005, An integration of GIS and remote sensing in groundwater investigations: A case study in Burdur, Turkey: Hydrogeology Journal, v. 13, no. 5–6, p. 826–834.
Shaban, A., Khawlie, M., and Abdallah, C., 2006, Use of remote sensing and GIS to determine recharge potential zones: The case of Occidental Lebanon: Hydrogeology Journal, v. 14, no. 4, p. 433–443, doi: 10.1007/s10040-005-0437-6.
Siddiqui, S.H., and Parizek, R.R., 1971, Hydrogeological factors affecting well-yields in folded and faulted carbonate rocks in central Pennsylvania: Water Resources Research, v. 7, no. 5, p. 1295–1312, doi: 10.1029/WR007i005p01295.
Singer, S.N., Cheng, C.K., and Scafe, M.G., 2003, Hydrogeology of Southern Ontario: Toronto, Ontario Ministry of the Environment, 200 p.
Singhal, B.B.S., and Gupta, R.P., 1999, Applied Hydrogeology of Fractured Rocks: Dordrecht, Kluwer, 399 p.

Solomon, S., and Quiel, F., 2006, Groundwater study using remote sensing and geographic information systems (GIS) in the central highlands of Eritrea: Hydrogeology Journal, v. 14, no. 5, p. 729–741, doi: 10.1007/s10040-005-0477-y.

Spitzer, R., 1981, Landsat and Seasat Data for Lineament and Lithologic Mapping in Southeastern Ontario [M.Sc. thesis]: Hamilton, Ontario, McMaster University, 190 p.

Sukhija, B.S., Reddy, D.V., Nagabhushanam, P., Bhattacharya, S.K., Jani, R.A., and Devender, K., 2006, Characterisation of recharge processes and groundwater flow mechanisms in weathered-fractured granites of Hyderabad (India) using isotopes: Hydrogeology Journal, v. 14, no. 5, p. 663–674, doi: 10.1007/s10040-005-0461-6.

Tam, V.T., De Smedt, F., Batelaan, O., and Dassargues, A., 2004, Study on the relationship between lineaments and borehole specific capacity in a fractured and karstified limestone area in Vietnam: Hydrogeology Journal, v. 12, no. 6, p. 662–673, doi: 10.1007/s10040-004-0329-1.

Therrien, R., and Sudicky, E.A., 1996, Three-dimensional analysis of variably-saturated flow and solute transport in discretely-fractured porous media: Journal of Contaminant Hydrology, v. 23, no. 1–2, p. 1–44, doi: 10.1016/0169-7722(95)00088-7.

Therrien, R., McLaren, R.G., Sudicky, E.A., and Panday, S.M., 2006, HydroGeoSphere: A three-dimensional numerical model describing fully-integrated subsurface and surface flow and solute transport: User manual: Waterloo, Ontario, Groundwater Simulations Group, 349 p.

Waters, P., Greenbaum, D., Smart, P.L., and Osmaston, H., 1990, Applications of remote sensing to groundwater hydrology: Remote Sensing Reviews, v. 4, no. 2, p. 223–264.

Wilson, M.E., 1961, Geology of Perth, Lanark and Leeds Counties, Ontario: Geological Survey of Canada Map 1089A, scale 1:63,000.

Wise, D.U., 1982, Linesmanship and the practice of linear geo-art: Geological Society of America Bulletin, v. 93, p. 886–888, doi: 10.1130/0016-7606(1982)93<886:LATPOL>2.0.CO;2.

Wise, D.U., Funiciello, R., Parotto, M., and Salvini, F., 1985, Topographic lineament swarms: Clues to their origin from domain analysis in Italy: Geological Society of America Bulletin, v. 96, p. 952–967, doi: 10.1130/0016-7606(1985)96<952:TLSCTT>2.0.CO;2.

Manuscript Received 9 April 2007
Revised Manuscript Received 21 February 2008
Manuscript Accepted 22 April 2008

Printed in the USA